KIST

LEADING THE WAY
TO A BRIGHTER FUTURE
THROUGH RESEARCH

MAIN RESEARCH FIELDS

- Future Fusion Technology
- Nano-Science
- Materials Science & Technology
- Intelligent Systems
- Energy & Environment
- Life Science
- Natural Products

KIST is working to turn your dreams into reality

미래를 여는 KIST
Korea Institute of Science and Technology

Cover story. *Endless Passion, Endless Movement, Endless Power*

Vol.2 No.1 January 2009

KISTtoday

Leading to the world of tomorrow

contents

Foreword

KIST is very pleased to release this second issue of KISToday in which we share the R&D activities and achievements of the institute with our global friends. The sharing of knowledge and experience among international partners, all of whom face common challenges in the 21st century, has become increasingly important to bring about the advancements in science and technology that will ultimately benefit culture and humanity in every part of the world.

At this time, the world is experiencing a severe economic downturn. The scale of this crisis and the speed at which it has spread clearly highlight the depth of interconnection among countries . Earlier lessons from the 1930's have taught us that science and technology can play a key role in overcoming economic crisis. A recent OECD STI working paper analyzed some of the best ways to achieve open global innovation. Its conclusions emphasized the importance of external partnerships, cooperate venturing and co-operative arrangement of R&D facilities among OECD countries. In this globally networked era, cooperation in science and technology through collaborative R&D activity across national borders should be the driving force for a prompt reversal of the current economic downturn.

In this issue, the technical aspects of a fuel cell powered by microbes is described as an example of the innovative technologies being pursued at KIST. Other topics include a look at air quality assessment using a unique smog chamber, design of metallic alloys with superior properties, novel metabolic techniques for identifying disease biomarkers, new approaches to nanowire production and its use in nano devices, and the development of increasingly seamless interaction between the real and virtual world through webized tangible space. We have featured these topics as ones of particular relevance in today's world and examples of the inspirational work taking place at our institute. We look forward to sharing further developments in our research efforts over the coming years.

January 2009
Dongwha Kum
President

Microbial Fuel Cell

B. Hong Kim
Center for Fuel Cell Research
●
hjkim25@kist.re.kr

(A)

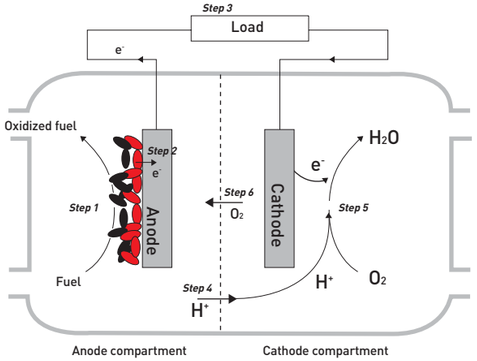

(B)

FIGURE 1. Schematic diagram (A) and photograph of the microbial fuel cell reactor.

A man carries more microbial cells in his body than the number of cells that make up his body. Microbes are everywhere thriving even under a variety of extreme conditions where higher organisms cannot. This is possible because of the wealth of genes, metabolic pathways and molecular processes that are unique to microbial cells. Among others some microbes can generate electricity while consuming organic contaminants in wastewater. A term "microbial fuel cell" (MFC) is used to describe a microbial device generating electricity. An MFC consists of anode and cathode separated by a cation specific membrane (Figure 1). The anode is inhabited by microbes that oxidize organic contaminants generating electrons, protons and carbon dioxide in the absence of oxygen. The cathode is aerated, the anode devoid of oxygen. Oxygen is reduced at the cathode consuming electrons transferred from the anode through an electrical circuit and protons diffused through the membrane. These reactions can be summarized as;

Anode reaction : $(CH_2O)_n + nH_2O \rightarrow nCO_2 + 4ne^- + 4nH^+$
Cathode reaction : $O_2 + 4e^- + 4H^+ \rightarrow 2H_2O$

1. HOW WE STARTED

Most microbes respire oxygen as their higher counterpart, but some replace oxygen with other oxidized compounds for their respiration. These include nitrate, sulfate, carbonate, halogenated hydrocarbons and oxidized metal ions. These compounds are referred to as electron acceptors. Metal ions used as electron acceptors by microbes include toxic heavy metals such as arsenate, chromate and selenate, and even radioactive metals found in wastewater from atomic power plants such as uranium(VI), technetium(VII) and neptunium(V) in addition to common metals such as Fe(III) and Mn(VI). They are extensively studied to develop processes to remove toxic metal ions from industrial wastewater containing them. We were not interested in those using water soluble metal ions as their electron acceptors,

Previously MFCs employed electron shuttle compounds that is reduced in the microbial cell and diffused out of the cell to be oxidized at the electrode surface.

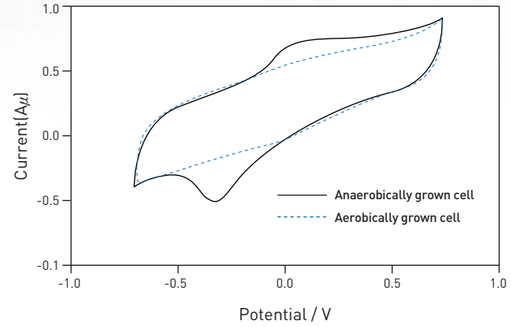

FIGURE 2. Cyclic voltammogram of an Fe(III)-reducing bacterium, *Shewanella putrefaciens* cell suspension.
The bacterium was cultivated with of without oxygen before washed and suspended in a pH buffer. The electrochemical activity of the cell suspension was measured using a potentiostat. Anaerobically grown cell suspension produced peaks that mean that the bacterial cells can exchange electrons with the electrode. This activity is believed due to the presence of electrochemically active compound on the cell surface that is needed to respire water insoluble Fe(III). Aerobically grown cells does not possess it to conserve more energy respiring oxygen.

but in Fe(III)-respiring bacteria. Water soluble electron acceptors used by microbes enter the microbial cells to comsume electrons within the cell. Fe(III) is a water insoluble electron acceptor, hence it does not enter the microbial cells. Instead those microbes using it as their electron acceptor export electrons to the cell surface to reduce the water-insoluble electron acceptor outside of the cells. A test was made to see if an Fe(III)-reducing bacterium, *Shewanella putrefaciens* can transfer electrons to a solid surface under conditions where oxygen is absent [1]. A simple electrochemical technique known as cyclic voltammetry showed that the bacterium can exchange electrons with an electrode (Figure 2). When cultivated in a fuel-cell type electrochemical device this bacterium generated electricity while consuming lactate. This was the first observation that a microbe passes electrons to an electrode on its own.
Previously MFCs employed electron shuttle compounds that is reduced in the microbial cell and diffused out of the cell to be oxidized at the electrode surface. These compounds are toxic, and MFCs using them found few areas of application. These results were presented at an American Chemical Society Meeting (Birmingham, AL., 9-11 September, 1996) as an invited lecture. This finding didn't attract an immediate attention but widely publicized later [2-3].

2. SELECTION OF BETTER MICROBES FROM NATURE

Since single microbes have limited capability to utilize organic contaminants, an electrochemical device used in the previous studies was employed to select microbial consortia generating electricity under various nutritional conditions ranging from artificial wastewater containing simple acetate to an actual wastewater. When

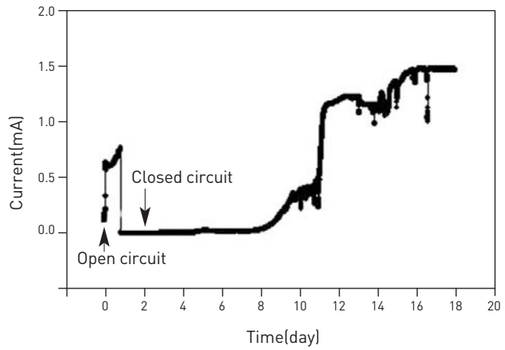

FIGURE 3. Potential differences between the anode and cathode of an MFC after inoculated with activated sludge and fed with wastewater.
Before the electrodes were not connected an open potential of about 0.8 volt was developed that was decrease to the base line when they were connected through a resistance of 10 ohm. The potential increased gradually to a stable level. The potential difference under the closed circuit can be converted to current based on the relationship of current = voltage/resistance.

wastewater was fed to the device inoculated with biomass collected from a wastewater treatment plant, a stable electrical current was obtained within 3 weeks after initial low current (Figure 3). The increase in current generation was coupled with changes in bacterial population that was analyzed by denaturant gradient gel electrophoresis of 16S ribosomal RNA genes amplified by polymerase chain reaction. The increase in current generation is due to the fact that the number of electricity generating microbes is small at the initial stage, and increases under the given conditions [4]. The term "enrichment culture" is used in microbiology to describe a process selecting a microbial population with desired properties. This enrichment culture technique became a standard procedure to start up a microbial fuel cell in many laboratories around the world [5].

3. MICROBIOLOGY OF MICROBIAL FUEL CELLS

An anode was removed from an MFC operated over a year for microbiological analyses. Microscopic observation showed the electrode is covered by well formed biofilm that consisted of microcolonies of Gram-negative bacteria and Gram-positive bacteria (Figure 4). Studies were made to characterize energy conservation process by the microbes in an enriched MFC through electrochemical analyses and use of respiratory inhibitors. It was found that the electricity generating microbial consortium conserves less than one third of energy carried by the contaminants consumed and that the remaining two thirds are used in electricity generation (Figure 5). This is an important aspect of MFCs as a wastewater treatment process (see below).

Microbial metabolism is regulated to obtain more energy under given conditions. As mentioned above microbes use various electron acceptors with varying degree of energy conservation. Oxygen is the best electron acceptor in terms of energy conservation followed by nitrate, metal ions, sulfate and carbonate. When anode of an MFC was added with oxygen or nitrate, current decreased concentration dependent manner [6]. When MFCs are used as a biochemical demand sensor this fact should be considered (see below).

Bacterial population was analyzed and compared between MFCs enriched with different nutritional conditions by culture-dependent and-independent procedures. Various bacterial groups were identified as the major constituents. This suggests that the electrochemical activity, the ability to generate electricity is widespread in the microbial world. There are some evidences to believe that the electrochemical activity is not directly related to the Fe(III)-reducing activity. The role of electrochemical activity of microbes in the natural ecosystem is an area of further studies.

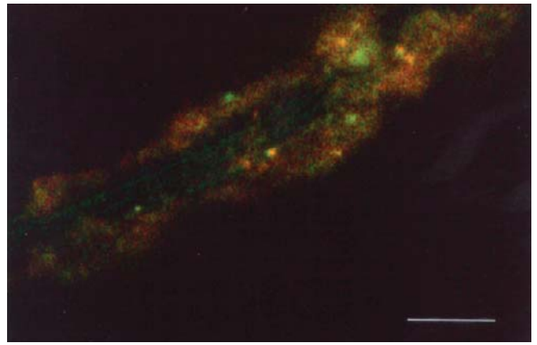

FIGURE 4. Confocal scanning laser micrograph of the biofilm on the anode. The electrode was stained red color for Gram positive bacteria and green for Gram negative bacteria.

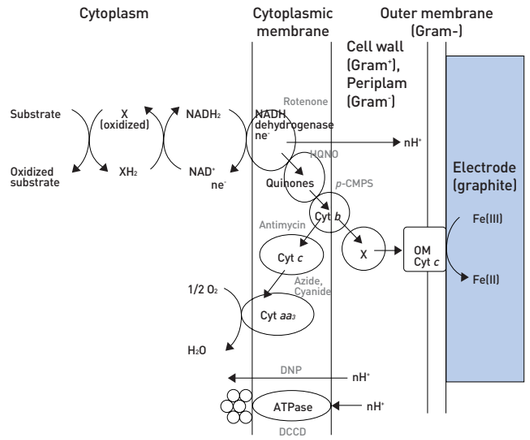

FIGURE 5. Proposed electron transfer from the bacterial cell forming biofilm on the anode to the electrode from the experimental results with respiratory inhibitors.

4. ELECTROCHEMISTRY OF MFCS

After a successful enrichment procedure was developed, studies were made to identify limiting factors in current generation and to optimize the performance of MFCs. When an MFC was run with different external resistance in batch mode operations, lower external resistance resulted in higher current that decreased rapidly with two shoulders (Figure 6). Based on these results proton diffusion from anode to cathode is the most serious limiting factor followed by oxygen supply to the cathode [7]. In electrochemistry these limitations are defined as internal resistances. Studies are being made to improve the performances of MFCs reducing the internal resistances around the world (see www.microbialfuelcell.org).

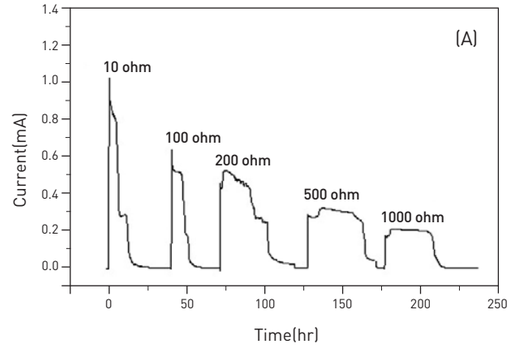

FIGURE 6. Current generation from an MFC operated in a batch mode with different external resistance.
With a resistance of 10 ohm current increased immediately after the addition of fuel and dropped with 2 shoulders that mean the current generation is limited by certain parameters. The first drop turned out to be due to the slow proton diffusion from the anode to the cathode, and the second due to the limitation of oxygen supply to the cathode. The high external resistances over 500 ohm limit the current generation.

5. WHAT CAN WE DO WITH MFCS

As stated above MFCs can generate electricity consuming organic contaminants. MFCs can be used as a novel wastewater treatment process concomitantly generating electricity. Since the current generate from MFCs are directly proportional to the concentration of contaminant in wastewater, they can be used to monitor the concentration of contaminants. The term "biochemical oxygen demand" (BOD) is used to evaluate the water quality, and BOD is a very important parameter in water industry.

5.1 MFCS TO TREAT WASTEWATER

Wastewater contains contaminants that deplete dissolved oxygen in water body that receives untreated one. Aquatic organisms including fishes need dissolved oxygen in water they live. This is the reason why wastewater should be treated before discharged. The conventional wastewater treatment is very expensive to install and to operate. Wastewater is aerated to supply oxygen for the microbes to oxidize organic contaminants. In average wastewater treatment consumes approximately 3-5% of the total electricity output in developed countries.

Microbes use the contaminants as their food to grow. The microbial cell grown is a secondary waste known as excess sludge to be disposed of. Since major part of energy carried by the contaminants are converted to electricity, excess sludge from MFCs can be reduced to about 20 % compared with the conventional wastewater treatment process. In addition electricity produced from MFCs can supplement energy needed in the process. A rough calculation showed that sewage treatment through MFC in EU can save 0.95 million ton of fossil fuel a year reducing the emission of CO_2, the greenhouse effect gas and over US$2.3 billion in the excess sludge disposal cost annually.

It is in an infant stage for the commercialization of MFC as a wastewater treatment process. MFC performance should be improved reducing the internal resistance. This needs considerable efforts in microbiology as well as in electrochemistry. A rough calculation showed that enough electricity can be generated to meet the consumption for 867 homes when wastewater from a town of 100,000 people is treated by MFC (see www.microbialfuelcell.org). It should be noted that this calculation does not consider energy required to run the system.

5.2 MFC AS A BOD SENSOR

BOD is the most widely used parameter to measure organic content in wastewater. The standard method to determine BOD involves the measurement of the dissolved oxygen consumed by microbes in the biochemical oxidation of organic matter. The BOD measurement has a number of limitations including irreproducibility, and is labor intensive and time consuming. It is therefore, not suitable for process control and real-time monitoring where rapid feedback is essential.

FIGURE 7. A BOD sensor using an MFC.

MFCs have been successfully used monitoring the real-time BOD values [8]. MFCs have been used not only to analyze wastewater but also low BOD values using MFCs enriched with river water containing low organic matter [9]. A BOD sensor

based on MFC have been successfully commercialized (Figure 7).

Since alternative electron acceptors such as oxygen and nitrate are preferentially reduced the signal becomes low when samples containing them are analyzed. Oxygen diffuses through the membrane into the anode chamber from the cathode side. Generally effluent from wastewater treatment plant contains high concentration of nitrate. Some respiratory inhibitors such as cyanide and azide were found to be useful to measure BOD accurately in the presence of oxygen and nitrate [10].

6. WHERE TO GO

MFC using electrochemically active microbes has a history of less than 15 years. This subject is under active investigation around the world. MFC has been successfully commercialized as a BOD sensor. It is speculated that MFCs will be exploited as a wastewater treatment process in near future to recover energy from waste.

When we started to work on the electrochemistry of Fe(III)-reducing bacteria, scientists at the US Naval Research Laboratory studied a two-electrode system to generate electricity oxidizing marine sediments [11]. This approach can not only power remote sensors at sea but also stabilize sediment in polluted lakes. "Mud battery" is the term used to describe this system. Microbes colonized onto an electrode buried in the anaerobic sediment layer oxidize organic contaminants transferring electron to another electrode placed in the aerobic water layer. This is an inexpensive technology to clean up polluted lakes harvesting electricity.

7. THOSE WORKED ON MFCS AT KIST

It should be emphasized that I have been very fortunate to have all those hard working good people as colleagues and students. It is them to be praised for the pioneering works on mediator-less MFC. Dr. D. H. Park who initiated the study as a PhD candidate is a professor at Seokyung University. Dr. H. S. Park had enriched an electrochemically active microbial consortium for the first time for his PhD degree. He is living in Canada. A post doctoral fellow Dr. H. Moon contributed the study in the engineering aspects. He is working in China. Postdoctoral fellows in early stage of the study were Dr. H. J. Kim, a professor at Kunkuk University and Dr. M. S. Hyun, CEO of Korea BioSystem Co, manufacturing MFC as BOD sensor. Dr. J. K. Jang of National Academy of Agricultural Science developed a membrane-less MFC as a part of her PhD thesis. Dr. C. A. Pham from Vietnam isolated and characterized an electrochemically active bacterium and Dr. B. C. Jong from Malaysia developed a thermophilic mediator-less MFC. There were several very productive MSc students; Ms Jiyoung Lee, Mr T. H. Pham, Ms Nguyet. T. Phung and Ms Pamela Y. F. Choo. Above all Dr. I. S. Chang who coordinated the projects should be credited. Dr. Chang is a professor at Gwangju Institute of Science and Technology.

REFERENCES

1. Kim BH, Kim HJ, Hyun MS, Park DH. 1999. *Journal of Microbiology and Biotechnology* 9: 127-31
2. Schubert C. 2006. *Nature* 441:277-79
3. Lucentini J. 2006. *The Scientist* 20:42-47
4. Lee J, Phung NT, Chang IS, Kim BH, Sung HC. 2003. *FEMS Microbilogy Letters* 223:185-91
5. Kim BH, Park HS, Kim HJ, Kim GT, Chang IS, Lee J, Phung NT. 2004. *Applied Microbilogy and Biotechnology* 63:672-81
6. Chang IS, Moon H, Jang JK, Kim BH. 2005. *Biosensors and Electronics* 20:1856-59
7. Gil GC, Chang IS, Kim BH, Kim M, Jang JK, Park HS, Kim HJ. 2003. *Biosensors and Electronics* 18:327-34
8. Kim BH, Chang IS, Gil GC, Park HS, Kim HJ. 2003. *Biotechnology Letters* 25:541-45
9. Phung NT, Lee J. Kang KH, Chang IS, Gadd G, Kim BH. 2004. *FEMS Microbilogy Letters* 223:77-82
10. Chang IS, Moon H, Jang JK, Kim BH. 2005. *Biosensors and Electronics* 20:1856-59
11. Tender LM, Reimers CE, Stecher HA, Holmes DE, Bond DR, Lowy DA, Pilobello K, Fertig SJ, Lovley DR. 2002. *Nature Biotechnology* 20:821-25

Gwi Nam Bae
Center for Environmental Technology Research
gnbae@kist.re.kr

Using a Smog Chamber as a Tool for the Characterization of Secondary Products in the Air

Smog is a visible air pollution phenomenon which occurs frequently in urban areas. The secondary oxidation products of organic gases and nitrogen oxides in ambient air under solar irradiation account for visibility reduction. A controlled and simulated reaction chamber, known as a "smog chamber," is a powerful tool for the characterization of chemical reaction mechanisms and secondary products. The smog chamber consists of a reaction bag, a light source, precursors (volatile organic compounds (VOCs) and nitrogen oxides), and monitoring instruments (Figure 1). Smog chamber experiments first began in the 1950's and have provided important data to determine the correlation between primary pollutants as precursors and secondary products, such as ozone and secondary organic aerosols. These smog chamber experiments have significant advantages over field studies in examining the contribution of aerosol chemical components to visibility and deriving empirical correlations between those mass concentrations and visibility.

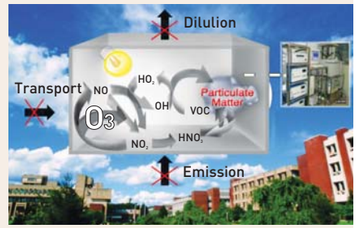

FIGURE 1. Conceptual diagram of a smog chamber.

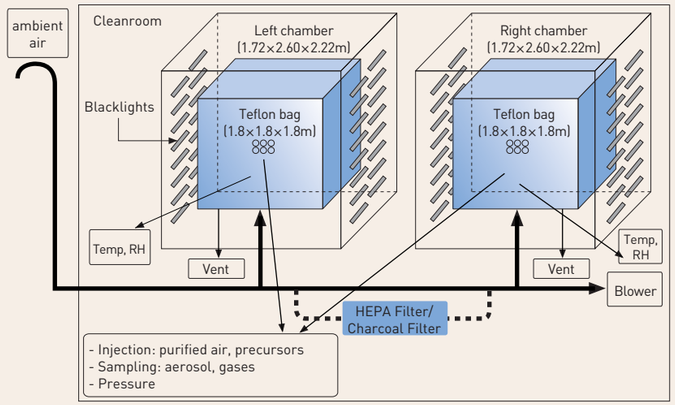

FIGURE 2. A schematic diagram of the twin smog chambers developed by KIST.

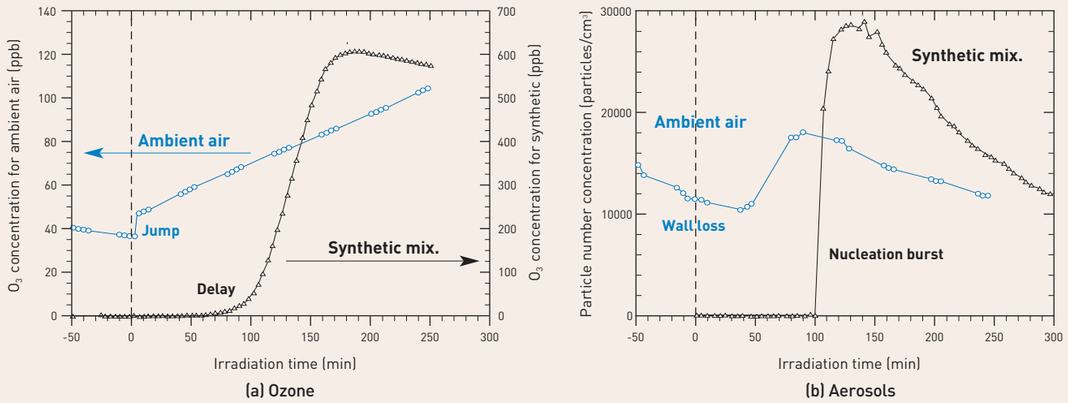

FIGURE 3. Comparison of synthetic mixture and ambient air experiments for ozone (a) and secondary aerosol (b) formation patterns.

Seoul is one of the smoggiest cities in the world. In looking for ways to alleviate this situation, KIST formed a smog research team which developed twin smog chambers to examine the real smog phenomena faced in the city (Figure 2). In each chamber, 64 blacklights were installed as light sources. Light intensity could be controlled by turning on different numbers of blacklights. The initial concentrations of aerosols and gases could be controlled by using a HEPA (high efficiency particulate air) filter or charcoal filter installed in the middle of the ambient air intake duct. These chambers were designed to simulate photochemical reactions of real ambient air as well as a VOCs-NO_x-air mixture. Since the photochemical reactions of real ambient air may be strongly dependent on initial urban air quality, the twin smog chambers permitted a comparison of data using the same initial urban air quality, thus excluding its effect and allowing a focus on critical underlying factors.

Typical smog chamber experiments have been conducted for VOCs-NO_x-air mixture or ambient air (Figure 3). For VOCs-NO_x-air mixture experiments, NO begins to convert to NO_2 immediately after the artificial light source is turned on. NO_2 is photolyzed into NO under irradiation, and NO reacts with O_3 to return to NO_2. The chemical process of ozone formation occurs when NO is converted to NO_2 by a reaction, not with O_3, but with other oxidants, such as organic peroxy radicals, which are formed through reaction sequences initiated by the reactions between the VOCs and hydroxyl radicals. When the concentration of NO_2 exceeds that of NO after enough irradiation, the VOCs (toluene) begin to be consumed rapidly and ozone starts to form simultaneously. Just after the onset of the ozone formation, secondary organic aerosols are formed due to gas-to-particle conversion processes. At first, the nucleation burst occurs under no seed particles. Thereafter, particles grow because condensational vapors, formed continuously, condense on the pre-existing particles. The secondary organic particles formed during the photochemical reactions in a smog chamber are almost spherical (Figure 4). For ambient air experiments, in contrast to the synthetic mixture experiments, hydroxyl radicals and aerosols already exist in ambient air. Therefore, ozone is formed shortly after irradiation and the nucleation burst of aerosols does not occur (Figure 3). From the smog chamber experiments, visibility reduction due to the formation of secondary organic aerosols could be estimated for real ambient air conditions (Figure 5).

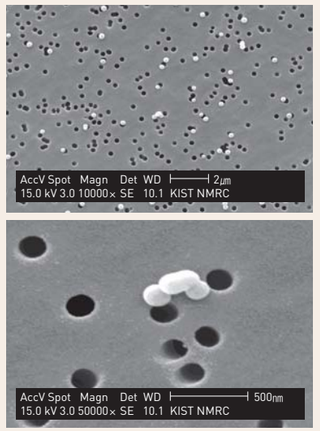

FIGURE 4. TEM images of secondary organic aerosols formed during the photochemical reactions in a smog chamber (KOSAE, 21, 2005, 27-38).

This smog chamber technique was applied to investigate the photochemical reactions of vehicle exhaust and to examine the ozone reaction with natural VOCs (α-pinene, *d*-limonene) emitted from a natural paint or air freshener. A significant amount of terpenes can be emitted from many types of building construction materials, air fresheners, and cleaning products. These terpenes can react with indoor ozone to form ultrafine particles and aldehydes. The ozone reaction chamber was set up to examine secondary pollution from a natural paint. Results showed that the number of ultrafine particles produced by a reaction between ozone and the terpenes emitted from a natural paint increased with increasing ozone concentration (Figure 6).

The KIST smog research team is involved in studies focused on finding sensitive parameters among primary pollutants (initial aerosols, toluene, α-pinene, NO_x, SO_2) and meteorological factors (light intensity, relative humidity, air temperature) which affect the ozone and secondary aerosol formations in real ambient air conditions. A further goal of the team is to derive a relationship between the light extinction coefficient of aerosols and these parameters. KIST's twin smog chambers are also being used to evaluate photochemical reactions of exhaust gases emitted from diesel vehicles both with and without diesel particulate filters, as well as LPG vehicles. Through these studies, KIST's research involving smog chambers is producing invaluable data for developing solutions to the urban smog problem.

KIST formed a smog research team which developed twin smog chambers to examine the real smog phenomena faced in Seoul.

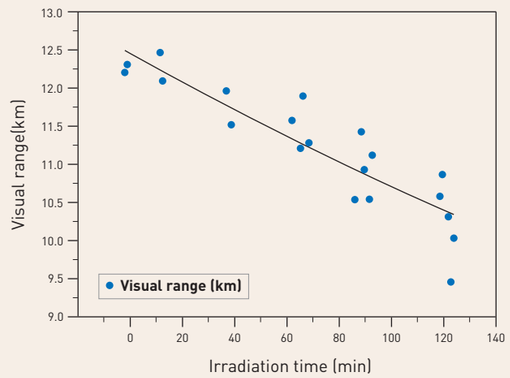

FIGURE 5. Change in visual range during the photochemical reactions in a smog chamber.

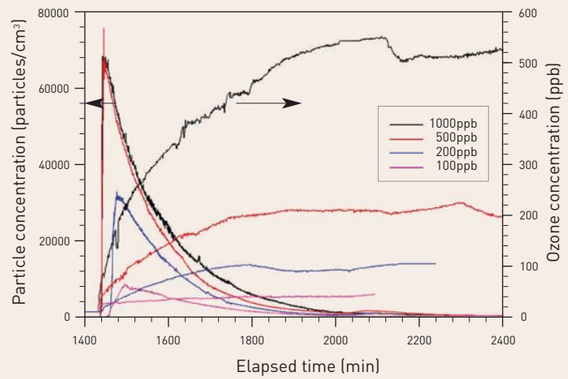

FIGURE 6. Change in particle number concentration during the ozone-initiated oxidations at different ozone concentrations of paint (Hazardous Materials, 141, 2007, 245-251).

Understanding Plastic Deformation in Metallic Glasses to Design New Alloys

Eric Fleury
Center for Advanced Functional Metals
●
efleury@kist.re.kr

Yu-Chan Kim
Center for Advanced Functional Metals
●
chany@kist.re.kr

Metallic glasses (MGs), first produced in 1960 by researchers from Cal Tech, are metallic alloys that lack crystallinity. Specifically designed to avoid the nucleation of the crystalline phase, the alloys preserve the disordering of the liquid melt, and are hence structurally amorphous (similar to oxide glasses). Though limited in size (~10 mm in diameter), MGs can be produced in alloy systems ranging from light alloys, such as Mg and Ti, to heavy metals, like Co, Fe and Ni, though Al still remains a challenge. The unique structure provides the MGs with exceptional physical (magnetic), chemical (corrosion), and mechanical (strength) properties, which make them attractive candidate materials for aerospace and advanced military applications, sporting goods, medical, electronic and micro/nano-electromechanical devices. While they can deform elastically (linear, reversible strain) up to ~2%, MGs are brittle. Under compression, their plastic deformation is limited to a few percent, due to plastic strain localization within thin shear bands (10-20 nm). The theory of dislocation developed by Volterra 100 years ago for metals is not applicable to MGs, and new concepts have to be proposed in order to understand the deformation behavior of these disordered metallic alloys.

Our approach has consisted of searching for correlations between structure and properties. The lack of information on the structure of MGs has been its major limitation so far. Figure 1 shows the mechanical behavior of binary Cu-Zr alloy and reveals the compositional dependency of strength and plastic deformation (1). Such compositional dependency was attributed to the change of the atomic packing of the alloys (2). Density measurements (experimental and molecular dynamics simulation) indicated that the maximum density attained for $Cu_{65}Zr_{35}$, and that densely packed alloys have maximum strength but limited deformation,

Molecular dynamics simulation) indicated that the maximum density attained for $Cu_{65}Zr_{35}$, and that densely packed alloys have maximum strength but limited deformation.

FIGURE 1. Composition-dependence of mechanical behavior

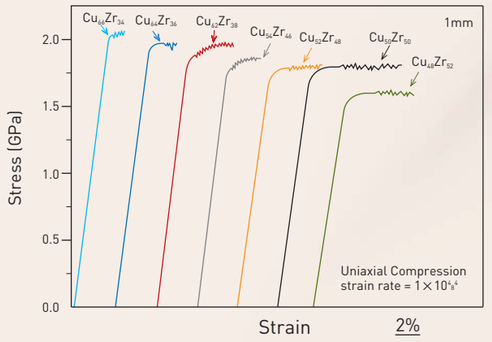

FIGURE 2. Variation of the fraction of Voronoi polygons with the Cu content

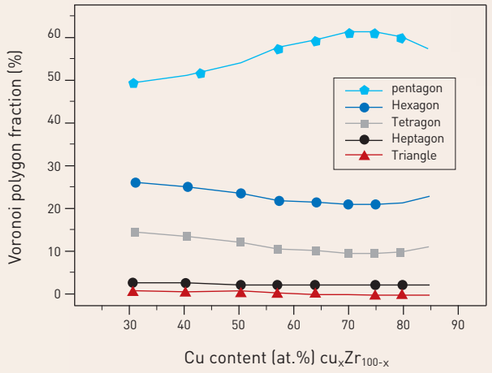

while alloys with a less-packed structure have less strength but can accommodate larger plastic deformation.

Using the Voronoi analyses on the simulated structure of Cu-Zr alloys, it is possible to gain information about the local atomic arrangement by looking at the near atomic neighbors. These analyses revealed the existence of different types of atomic clusters in Cu-Zr MGs. Though wide varieties of clusters are formed, some types of clusters are encountered more often than others; as seen in Figure 2, the volume fraction of icosahedral cluster defined by a 2-D pentagon with the index (0 0 12 0) is relatively high in the $Cu_{65}Zr_{35}$ alloy but lower in the $Cu_{50}Zr_{50}$. Icosahedron being a dense cluster, it would be expected that a structure with a high fraction of icosahedrons should be the densest.

However, if the cluster fraction is an important parameter to explain the strength, the spatial distribution of the cluster is believed to play a major role in the ability of the material to deform plastically, since it governs the atomic mobility. Recently Argon and Kuo developed the concept of the shear transformation zone (STZ) to explain the shear localization [3]. Under stress, one cluster (size of ~ 30 to 100 atoms) deformed elastically until it reached a jammed state where it flowed. The jammed STZ affects the surrounding material and eventually triggers the autocatalytic formation of shear bands. The molecular dynamic simulation of Cu-Zr shows that under applied shear stress, the local strain is not uniform owing to the spatial distribution of clusters of different symmetries (Figure 3). Regions with a high fraction of icosahedral (highly packed and strong clusters) do not deform much, while regions rich in clusters of lower packing undergo larger deformation. These deformed regions resemble the so-called STZ.

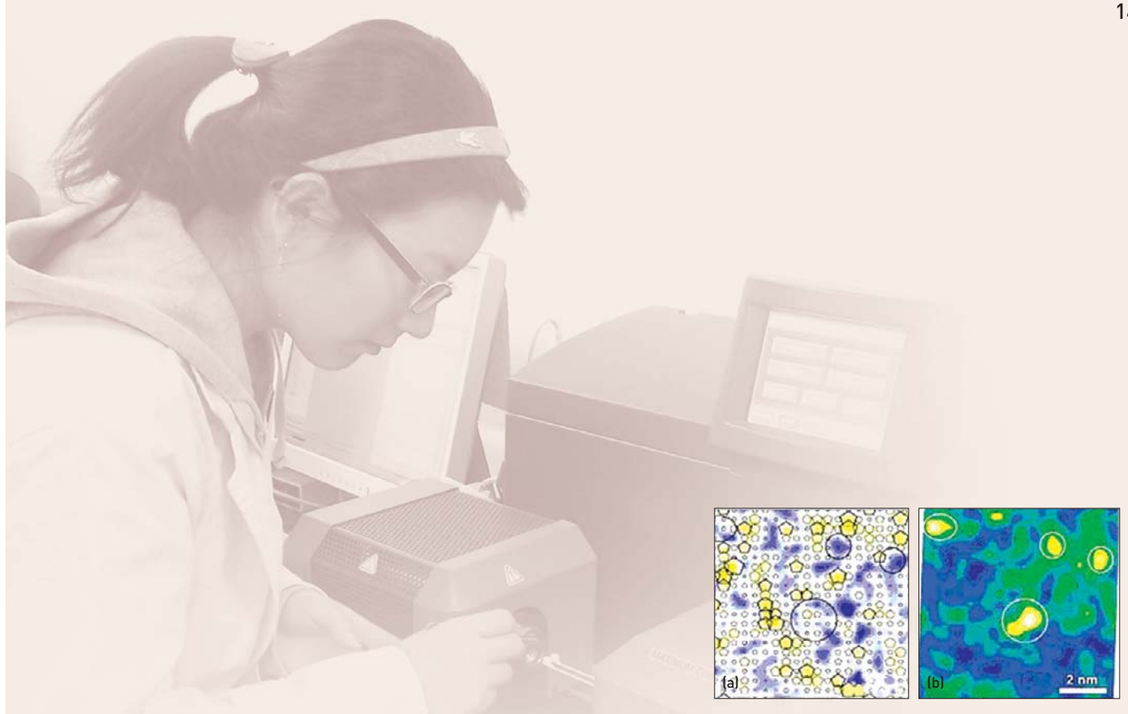

Tailoring properties is possible by controlling the local atomic structure of MGs. In particular, the introduction of loosely packed structures could be used to enhance plastic deformation. New MGs were thus designed using the concept of phase separation. Knowing that Cu and Ag tend to separate in the liquid phase, we created $(Cu_{50}Zr_{50})_{100-x}Ag_x$ and $(Cu_{50}Zr_{50})_{100-x-y}Al_xAg_y$ MGs, which gave experimental results indicating remarkable properties in terms of plastic deformation (Figure 4). The interface produced by the separation of the amorphous phases of different compositions introduces regions of lower atomic packing that promote a large number of STZs to trigger numerous shear bands, which delocalized shear strain into a larger volume of the MGs. The concept of phase separation appears to be an attractive route for the design of MGs with superior properties.

FIGURE 3. (a) Distribution of icosahedral clusters in $Cu_{53}Zr_{45}$; (b) distribution of local shear strain during shear deformation (yellow regions correspond to those undergoing large strain)

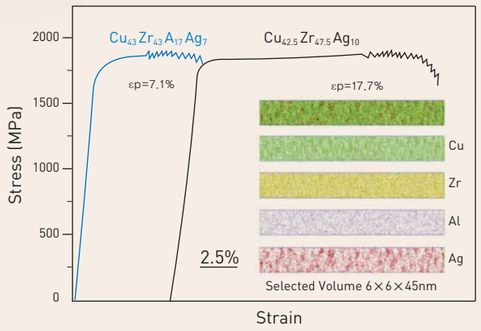

FIGURE 4. Mechanical behavior of Cu-Zr-Ag and Cu-Zr-Al-Ag and 3D-AP showing the phase separation in $Cu_{43}Zr_{43}Al_7Ag_7$

REFERENCES

1. Kwon OJ, Lee YK, Park SO, Lee JC, Kim YC, Fleury E. 2007. *Materials Science and Engineering A* 449-451:169-71
2. Lee JC, Fleury E, Lee BJ, Wakeda M, Shibutani Y. 2007. *Journal of Materials Research* 22:3087-97
3. Argon AS, Kuo HY. 1979. *Materials Science and Engineering* 39: 101-09
4. Oh JC, Ohkubo T, Kim YC, Fleury E, Hono K. 2005. *Scripta Materialia* 53:165-69

Metabolomic Approaches in Biomarker Discovery

Bong Chul Chung
Bionalysis & Biotransformation Research Center
●
bcc0319@kist.re.kr

In 2005, MIT's Technology Review introduced "metabolomics," a field expected to make a huge splash as an emerging technology. In contrast to classical bio-analyses that mainly focus on single metabolites and/or defined sets of linked reactions and cycles, metabolomics involves the collection of quantitative signatures on a broad series of metabolites to understand metabolic dynamics associated with biological conditions of interest. Since many diseases have metabolic fingerprints, metabolomics researchers are looking for metabolic biomarkers by analyzing more than 1,000 molecules in various biological specimens obtained from patients. There are technically two different strategies: ① targeted metabolite profiling, which is restricted to quantitative analysis of a class of compounds that are responsible for a specific pathway, as well as of the activities of related enzymes; and ② non-targeted metabolite profiling, which involves rapid and qualitative analysis of a large number of different metabolites to uncover potent biomarkers. A metabolomic protocol containing both targeted and non-targeted metabolite profiling techniques is summarized in Figure 1. Biological samples (e.g., urine, blood, tissue biopsies, or hair) are collected, pretreated for metabolite extraction, and analyzed with either gas chromatography-mass spectrometry (GC-MS) or liquid chromatography-mass spectrometry (LC-MS). The combination of these two techniques can also be used to gather more metabolites with a wide range of chemical and physical properties. For non-targeted metabolite profiling, the raw data was first collected and calibrated for unbiased and unsupervised comparisons of data sets, which are responsible for the correction of the baseline of ion traces in the raw data. After the alignment of all MS peaks to generate ordered data matrices, the mass ion amplitudes of the aligned peaks were examined and matrices were arranged. The latter were further examined by multivariate data analysis (MDA). A database was then generated to consider individual sample properties of the metabolites as potent metabolic biomarkers. Statistical analyses can be conducted to identify biological signatures, predict class from unrecognized groups in the data, identify interactions among variables, and network variables to understand biochemical metabolic changes. In similar fashion, quantitative results obtained from targeted metabolite profiling, which are suitable for more routine applications, can be directly compared within samples and introduced as metabolic biomarkers.

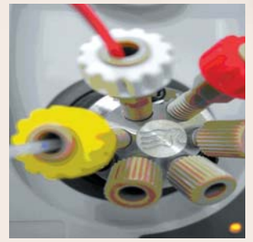

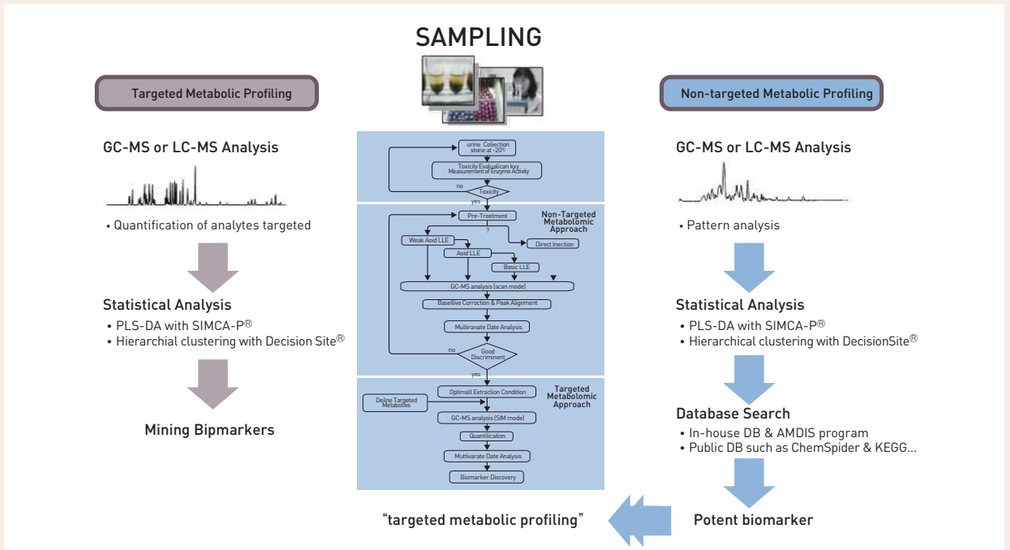

FIGURE 1. The flow diagram for chromatography-mass spectrometry based metabolomic approaches. Adapted and modified from *Anal. Chem.*, 79: 6102-6110, 2007.

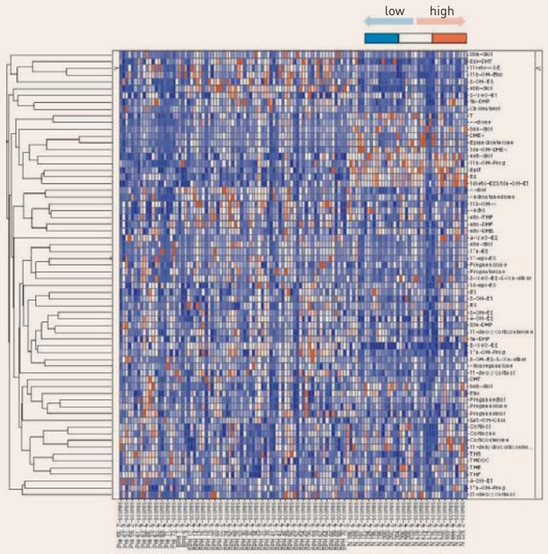

FIGURE 2. A metabolic signature of steroid hormones prepared by quantitative GC-MS analysis manipulated by multi-variate data analysis. This technique has been validated and successfully applied to biological samples to discriminate between subjects. The figure shows steroid hormones with altered concentrations in urine samples from human subjects. Each row represents a steroid and each column represents a subject, with each colored square representing the relative concentration of a single steroid in a single subject.

Abnormalities in steroid hormones are responsible for the development and prevention of many endocrine diseases. Due to their biochemical roles in the endocrine system, quantitative evaluation of steroid hormones is needed to elucidate altered expressions of steroids. Endogenous steroids that are part of the endocrine system (which, is involved in controlling human body functions) can be divided into five groups: androgens, estrogens, corticoids, progestins, and sterols. These are generally synthesized from cholesterol in the adrenal cortex, ovaries, and testes in biological enzyme activities. Here, we introduce a multi-enzyme monitoring technique. Although enzyme activities have been monitored by the reaction of the targeted enzyme with a substrate molecule, over-estimation of radioimmunoassay and enzyme immunoassay have limited these assays because of cross-reacting antibodies and the measuring of only a single compound at a time. The quantitative analysis of endogenous urinary steroids, including 22 androgens, 18 estrogens, 15 corticoids, 13 progestins, and 2 sterols, by GC-MS combined with statistical analysis is introduced here. Our study focuses on explaining the activities of enzymes correlated with whole steroidogenesis; enzyme activity may be a useful tool for clinical diagnosis as well as a mining biomarker in hormone-dependent diseases. A novel aspect of this study is the introduction of the "metabolic signature," which expresses different enzyme activity related to different diseases. It might then assess the relationship between steroid metabolism and diseases from multiple enzyme array data based on quantitative results with important prognostic implications (Figure 2).

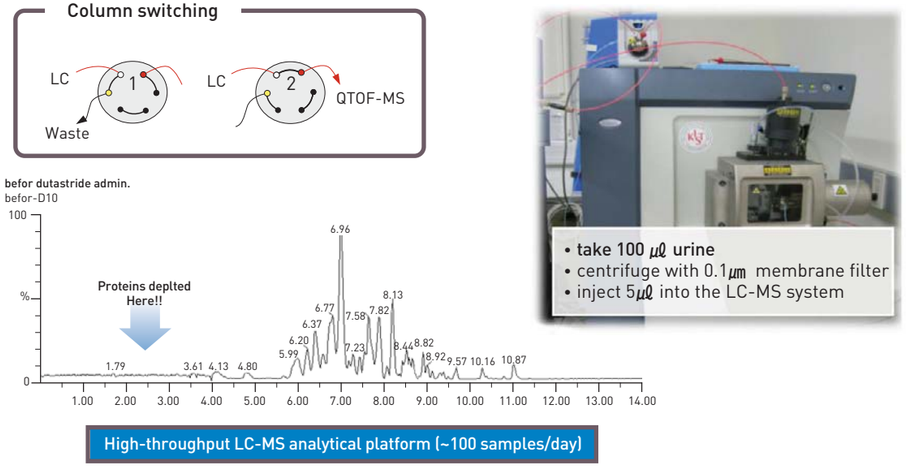

FIGURE 3. A platform for high-throughput, non-targeted, metabolite profiling. For sample preparation, 200μℓ of urine filtered with Ultrafree-MC Durapore (PVDF, 0.1μm × 0.5 mℓ) were injected directly into a hybrid column (Cadenza HS-C18, 2.0 mm i.d. × 100 mm, 3μm particle size) at a flow-rate of 400μℓ/min to isolate endogenous interferences, such as proteins and other macromolecules.

In contrast to targeted analysis, non-targeted metabolite profiling involves a large number of different metabolites with the objective of identifying a specific metabolite responsible for biological changes. A rapid and reproducible sample preparation procedure is necessary in non-targeted metabolomics because it may affect reproducibility as a result of the heterogeneity of metabolites derived from cell populations. A novel, non-targeted metabolite profiling technique using a hybrid stationary phase liquid chromatography (LC) column is coupled to a quadrupole-time-of-flight mass spectrometer (Q-TOF-MS) to identify altered metabolites and to find potential biomarkers (Figure. 3). Both the retention time and the spectral data for each chromatographic peak were paired and normalized with the ion intensities in data processing. All data processed were then statistically analyzed by partial least-squares discriminant analysis (PLS-DA) and hierarchical clustering analysis (HCA).

For comprehensive metabolomic approaches, both metabolite profiling techniques were conducted to find mining biomarkers (Figure 4). Two known biomarkers in breast cancer, i.e. 5-hydroxymethyl-2-deoxyuridine and 8-hydroxy-2-deoxyguanosine, were confirmed using the presented methods. In addition, three potential biomarkers for ovarian cancer, i.e. 1-methyladenosine, 3-methyluridine, and 4-androstene-3,17-dione, found in significantly increased levels using one-way variance analysis ($p < 0.05$), were identified as quantitatively targeted metabolites with pattern analysis. The cancer markers identified in this study are confirmed as metabolites closely associated with oxidative DNA damage and DNA methylation processes.

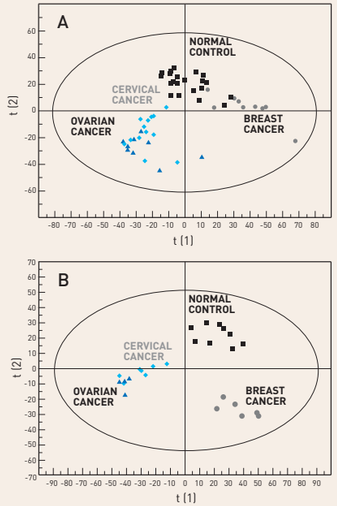

FIGURE 4. Non-targeted metabolite profiling was conducted for normal controls and for patients with breast, cervical, and ovarian cancers using PLS-DA (**A**). The X-axis, t[1] and Y-axis, t[2] represent the highest two X-scores of dimensions 1 and 2 for matrix X of mass ion abundances, respectively (**B**). Their metabolite patterns were fully distinguishable ($R^2Y = 0.299$, $Q^2Y = 0.200$), except that the profiles of patients with cervical and ovarian cancers were not distinguishable. (Black square: normal controls; red circle: breast cancer patients; blue triangle: ovarian cancer patients.) Adapted from *Clin. Chim.* Acta, 400: 63-69, 2009.

Nanowires as Ideal Building Blocks for Nano-Devices

Jae-Gwan Park
Nano-Materials
Research Center
●
jgpark@kist.re.kr

MIT's *Technology Review* in 2004 proclaimed nanowires as one of ten emerging technologies that would change the world, and in 2005 added quantum wires to that list. It was noted that nanowires are very versatile compared to other nanostructures because so many different properties can be achieved simply by varying the wires' composition. Ever since nanowires attracted renewed interest in the mid-1990s, there has been an explosion of research on the synthesis of nanowires and on related applications. Examples of the latter include gas/optical/bio sensors, field-effect transistors, solar cells, and nano-generators.

One-dimensional (1D) nanostructures can be synthesized by various techniques, including a template-assisted route, vapor-based methods, and wet chemistry. In the template-assisted approach, the template simply serves as a scaffold within which different materials are generated *in situ* and shaped into a nanostructure with a morphology complementary to that of the template. A variety of templates have been demonstrated successfully, with notable examples including step edges on the surfaces of a solid substrate, channels within a porous material, mesoscale structures self-assembled from organic surfactants or block copolymers, and existing nanostructures synthesized using other approaches. It is generally accepted that template-assisted synthesis provides a simple and cost-effective procedure. As a major drawback, nanostructures synthesized using template-directed methods are often polycrystalline and the quantity that can be produced in each run of synthesis is relatively small, limiting the number of applications for the resulting nanostructures.

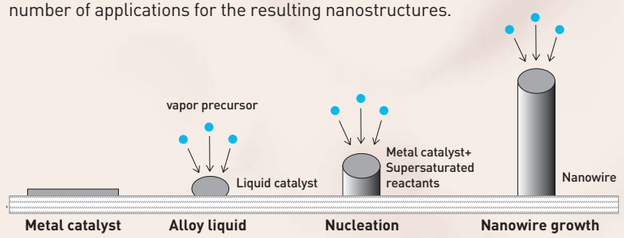

FIGURE 1. Schematic illustration for the growth of a nanowire via the VLS mechanism.

Among all vapor-based methods, the vapor-liquid-solid (VLS) process seems to be the most successful for generating nanowires with single-crystalline structures and in relatively large quantities. This process was originally developed by Wagner *et al.* to produce micrometer-sized whiskers in the 1960's and was recently revisited to generate 1D nanostructures from a rich variety of inorganic materials. Figure 1 shows the schematic illustration of the typical VLS process. As a major requirement for this process, a good solvent capable of forming a liquid alloy with the target material should exist. Ideally, the solvent and the target material should be able to form eutectic compounds. The process starts with the dissolution of gaseous reactants into nanosized liquid droplets of a catalyst metal. Once liquid droplets become supersaturated with the reactant, nanowire growth will start to occur at the solid-liquid interface, followed by nucleation and growth, first of single-crystalline rods and then of wires. The 1D growth is mainly induced and dictated by the liquid droplets, the sizes of which remain essentially unchanged during the entire process of wire growth.

VLS-grown 1D nanostructures are regarded as ideal building blocks for nano-devices because of unique properties such as excellent single crystallinity, easy carrier injection, a relatively easy doping, and a large surface-to-volume ratio. These properties have been demonstrated in a single-nanowire-based solar cell, a piezoelectric nano-generator based on individual/multiple ZnO nanowires, field-effect transistors, light-emitting diodes, logic circuits, and sensors. However, active devices such as transistors or diodes require a delicate e-beam lithography process and careful alignment. Thus, these devices have a long way to go for practical device applications. On the other hand, passive devices, like gas or photo sensors, can be fabricated using a relatively easier method.

Figure 2 shows a scanning electron microscopy (SEM) image of CdS_xSe_{1-x} alloy nanobelts (Figure 2(a)) and the fabrication procedure for an optical sensor (Figures 2(b) and (c)). CdS_xSe_{1-x} alloy nanobelts were synthesized on Au-catalyzed Si substrates by pulsed-laser deposition (PLD) via a VLS mechanism. We were able to obtain well-developed CdS_xSe_{1-x} alloy nanobelts on the down-stream side of a quartz-tube furnace after ~ about 10 minutes of laser ablation. Photoluminescence (PL) and x-ray diffraction (XRD) measurements revealed that the bandgap energy of CdS_xSe_{1-x} alloy nanobelts increased linearly depending on the S composition, implying that CdS and CdSe formed a complete solid solution within the nanobelts without any phase separation or secondary phases. As seen in Figures 2(b) and (c), we fabricated optical sensors by dispersing CdS_xSe_{1-x} alloy nanobelts on pre-fabricated Au electrodes. Figure 2(e) shows the normalized responsivity of a $CdS_{0.5}Se_{0.5}$-nanobelt optical sensor. Photons, whose energy is larger than the bandgap energy E_g of $CdS_{0.5}Se_{0.5}$, can generate electron-hole pairs contributing electrical current, but photons with lesser energy than the E_g do not generate any electron-hole pairs.

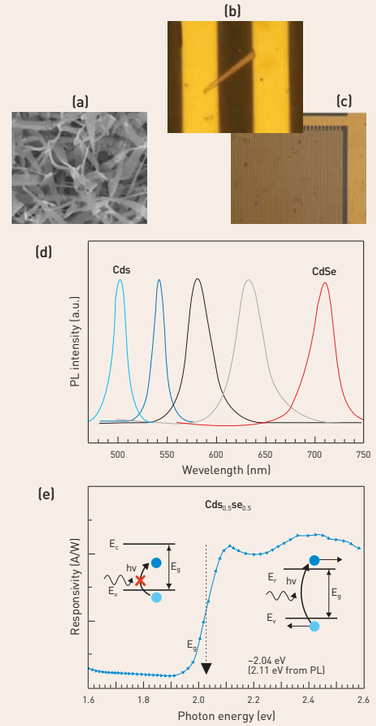

FIGURE 2. Synthesis, fabrication, photoluminescence (PL) and photo-current measurement of an optical sensor based upon CdS_xSe_{1-x} alloy nanobelts. [*Nanotechnology*, Vol. 17, 3775-3778 (2006); manuscripts on optical sensors in preparation]

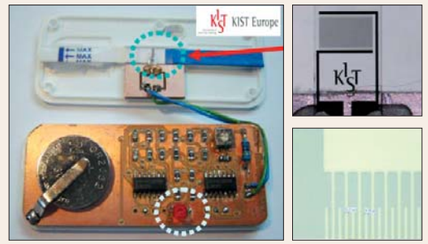

FIGURE 3. Rapid test kit integrated with a CdS_xSe_{1-x}-nanobelt optical sensor.

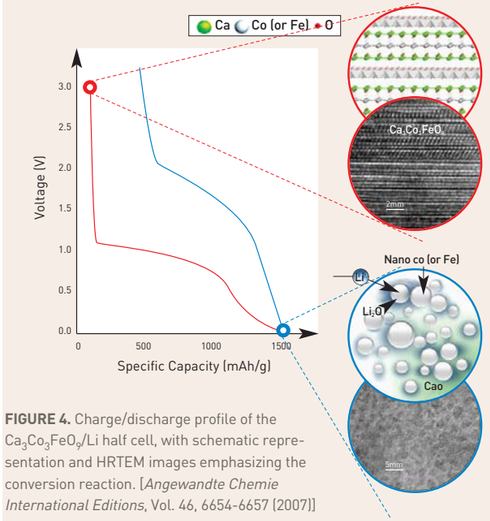

FIGURE 4. Charge/discharge profile of the $Ca_3Co_3FeO_9$/Li half cell, with schematic representation and HRTEM images emphasizing the conversion reaction. [*Angewandte Chemie International Editions*, Vol. 46, 6654-6657 (2007)]

Taking advantage of the excellent responsivity of a CdS_xSe_{1-x}-nanobelt optical sensor, we integrated the sensor into a bio-chip for detecting very weak luminescence or fluorescence resulting from an antigen-antibody reaction. To fabricate the bio-chip, as seen in Figure 3, a specific antibody was treated with luminescent/fluorescent agents, followed by immobilization on a test pad, onto which several drops of body fluid containing antigen were dropped. We successfully demonstrated the capability of a rapid test kit integrated with a nanobelt optical sensor against a pregnancy test, which showed a sensitivity more than 100 times higher compared to a commercial rapid test kit based on color reaction. Currently, we are working on applying a rapid test kit integrated with a nanobelt optical sensor to diseases, such as myocardial infarction and Alzheimer's, that require very high sensitivity due to the need for detection in their initial stages.

The design of nano-sized electrodes is one of the attractive strategies to develop high performance lithium ion secondary batteries that require high energy density, high power density, and long-term cycle stability for industrial applications. In particular, much attention has been focused on the nanostructuring of transition metal oxides (Co_3O_4, CuO, Fe_3O_4 etc.) and lithium alloy metals (Si, Ge, Sn) because they exhibit extraordinarily high storage capacities gained through reaction mechanisms different from classical insertion/deinsertion methods. Our group has reported on two novel anode materials that were successfully fabricated by ① a sol-gel method and ② a thermal evaporation process.

First, calcium cobaltite and iron-doped calcium cobaltite nanoplates, with average lateral sizes below 50 nm, were synthesized. It was clearly observed that $Ca_3Co_4O_9$ has a layered crystal structure, which is built up from the stacking along the c-axis of alternating triple rock-salt-type layers of $[CaO\text{-}CoO\text{-}CaO]_\infty$ and single CdI_2-type layers of $[CoO_2]_\infty$. The $Ca_3Co_4O_9$ nanoplate electrode demonstrated high reversibility and superior cycle stability. During the first discharge, $Ca_3Co_4O_9$ decomposed into active Co nanograins surrounded by the Li2O amorphous part and by an inactive CaO "spectator" matrix. This inactive CaO matrix contributes to reversibility retention by alleviating the mechanical stress induced by the volume change of the active part and by suppressing the aggregation of active nanograins upon subsequent cycling.

Second, we synthesized SnO_2/In_2O_3 heterostructured nanowires, which consisted of a core SnO_2 tetragonal phase and a shell In_2O_3 cubic phase. The latter phase has shown a considerable increase in lattice parameter by means of Rietveld refinement of the X-ray diffraction pattern due to incorporation of Sn into In_2O_3 during nucleation and growth. This incorporation results in the effective formation of ITO (In-doped tin oxide), consequently leads to 2-order-of-magnitude higher electron transport properties than are demonstrated by pure SnO_2 nanowires. These heterostructured nanowires exhibit even higher reversible storage capacities than pure SnO_2 nanowires since a highly conductive path is provided by the ITO shell structure.

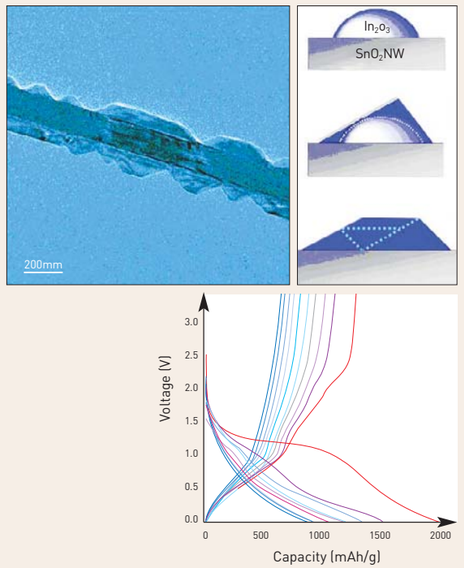

FIGURE 5. Low magnification TEM image, schematic growth mechanism, and charge/discharge profiles of SnO_2-In_2O_3 heterostructured nanowires. [*Nano Letters*, Vol. 7, 3041-3045 (2007)]

Tangible Web: Webized Tangible Space

Heedong Ko
Imaging Media Research Center
●
kol@imrc.kist.re.kr

Hyoung-gon Kim
Imaging Media Research Center
●
hgk@imrc.kist.re.kr

Humans are spatial beings, moving around in space and configuring the surrounding environment according to their needs. New kinds of spatial interactions are afforded by changes in the computing environment, whereby the physical environment is augmented with sensors and devices that can render and display images. We call this new interactive environment "Tangible Space," a term describing the seamless combination of the digitally augmented physical environment and the physically immersive and persistent virtual environment [1-2]. In Tangible Space we are building a virtual world that mirrors the physical environment, a world where we can not only see objects with their shapes and their spatial relations, as we can in the physical environment, but where we can also interact physically with those objects.

Likewise, humans are social beings, interacting with each other and sharing experiences through communication media like telephones, and more recently, through the World Wide Web ("the Web"). With rapid advancements in high speed wireless networks and mobile phones, the Web is becoming a social medium for sharing texts, photos, video, audio and experiences in general. If Tangible Space can be shared through the Web, we can not only interact with virtual objects as in a physical environment, but can also share our experiences in the physical environment, virtually, with our family and friends. We call such a webized Tangible Space "Tangible Web"[3].

To demonstrate the concept, we are developing a virtual replica of the KIST campus with buildings and roads that are aligned and scaled to mirror the physical KIST campus, as shown in Figure 1. Using this mirrored campus, a mobile user can become familiar with the campus before a visit and can even leave messages in places and on objects in the mirrored campus. Because the virtual campus mirrors the actual KIST campus, a mobile user in the physical environment is able to receive location-based services.

FIGURE 1. Mirrored KIST Campus
(a) View of KIST main building
(b) View of KIST pond.

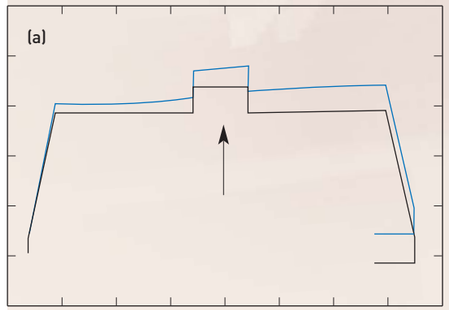

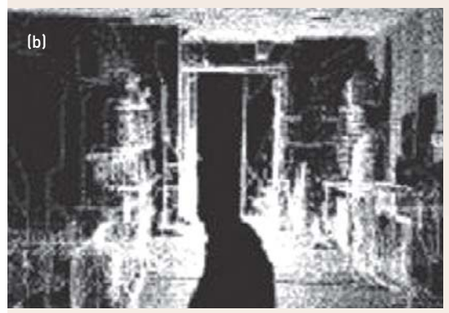

FIGURE 2. Indoor Mirrored World: (a) point cloud generation from a moving laser scanner with motion correction; (b) rendering of point cloud

Up to now, we have been building the mirrored KIST campus manually using graphic tools; however, we are currently developing an automatic modeling method for physical environments that is fast and accurate using planar laser scanners on a mobile platform. Figure 2 shows a preliminary result of mirroring an indoor office using this technique. In the coming year, we are planning to extend this method to outdoor environments like the KIST campus.

To stay current, the mirrored world must reflect changes in its physical counterpart in real time so that a user experiences the same world either virtually or physically . This is becoming possible with the real time mirroring techniques described above, as well as with the development of smart environments embedded with networked sensors. An additional requirement for the mirrored world is that it should be persistent, like its physical counterpart: that is, once made, changes should remain in place. However, one important difference between virtual and physical worlds is spatial accessibility. A mirrored world allows the user to connect to the internet and access it anywhere, while the physical world can only be accessed *in-situ*. Another difference is temporal accessibility where important events occurring in the physical environment may be logged in the persistent mirrored world and accessed in the future.

Seamless integration of the physical and mirrored worlds allows a person carrying a mobile device to annotate places or physical objects (*in-situ* annotation) in the real environment. These annotations can be shared with others by uploading to the persistent mirrored world. Figure 3 (a) shows annotations of the mirrored KIST campus and Figure 3 (b) shows them on the physical wall in an indoor office.

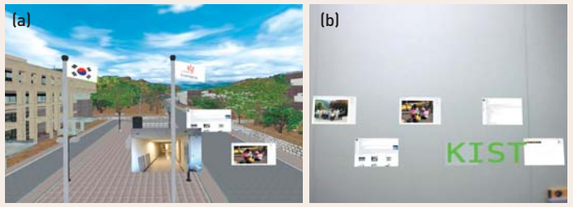

FIGURE 3. *In-situ* annotation of Tangible Space: (a) Annotation of mirrored KIST model; (b) Annotation of physical environment

An annotated web page is rendered on a web board where a user may issue a request to get a document through HTTP URI. Using URI as an address, the web board connects to the web server where the document is located and retrieves the document. The web boards may then be attached to objects and placed in the mirrored world. The annotated pages can be retrieved in the mirrored world's physical counterpart if the user's position has been tracked as a location-based service.

The Tangible Web can be browsed using many types of tangible interaction methods. Figure 4 shows two forms of interaction with Tangible Webs. Figure 4 (a) shows that a user could browse multiple web pages in a 3D immersive virtual environment, and Figure 4 (b) shows a mobile user looking at a physical camera where the web documents associated with the camera are automatically retrieved and overlaid with multiple options and with additional information about the product. In addition, we are also considering applications involving a multi-touch worktable whereby multiple users can share Tangible Web contents physically with one device.

Figure 4 suggests interesting uses for the Tangible Web, but we believe the ultimate Tangible Web application would be a lifelog service [4-5]. That is, a person wearing or carrying powerful computing devices, such as smart phones, could log his/her daily life into a Tangible Web. Since these personal devices are interwoven with those of other users through the web, users can share their experiences with each other. As a lifelog system can archive personal history, context aware services based on this temporal information can be exploited. We define the Tangible Web as follows:

- Web with Tangible Interaction (Immersive Web)
  - Real-time information archiving and rendering for more immersive cyber space
  - Augmented, mixed, virtual reality with wearable devices
- Web linked with the real world (Real World Web)
  - Seamless integration of the Web with the real world context based on the specific location, activity or user context in the real world
  - Ubiquitous smart object and sensor networks
- Web with User Experience (Experience Web)
  - Context and contents from user experience
  - Practical approach of the context-aware semantic web

For now, the concept of the Tangible Web remains vague and there is little experience in how other new web technologies, such as web 2.0 or semantic web could be applied and serviced in the Tangible Web. However, we are confident that KIST's Tangible Web research will generate innovative ideas and visionary approaches that will help shape the future development of the next World Wide Web.

FIGURE 4. Tangible web: (a) Immersive Tangible Web; (b) Mobile Tangible Web

REFERENCES

1. Sylvia Irawati, Sang-chul Ahn, Jinwook Kim, and Heedong Ko, "VARU Framework: Enabling Rapid Prototyping of VR, AR and Ubiquitous Applications," IEEE Virtual Reality, Reno, March 2008.
2. Jane Hwang, Sangyup Lee, Sang Chul Ahn, Hyoung-gon Kim, "Augmented Robot Agent: Enhancing Co-Presence of the Remote Participant," IEEE and ACM International Symposium on Mixed and Augmented Reality, September 2008
3. Jinwook Kim, Yong-Moo Kwon, Hyoung-gon Kim, and Heedong Ko, "Tangibleweb: filling the gap between virtual and real worlds," Asiagraph 2008, Japan, October 2008.
4. Ig Jae Kim, Sang Chul Ahn, Heedong Ko, and Hyoung-Gon Kim, "Automatic Lifelog Media Annotation based on Heterogeneous Sensor Fusion," IEEE International Conference on Multisensor Fusion and Integration for Intelligent Systems, August 2008.
5. Ig-Jae Kim, Sang Chul Ahn and Hyoung-gon Kim, "Experience Sharing in Tangible Web on Lifelog," Asiagraph 2008, Japan, October 2008.

PUBLICATIONS

1 A Serial Dilution Microfluidic Device Using a Ladder Network Generating Logarithmic or Linear Concentrations

Lab on a Chip 8, 2008, 473–479

Choong Kim, Kangsun Lee, Jong Hyun Kim, Kyeong Sik Shin, Kyu-Jung Lee, Tae Song Kim and Ji Yoon Kang

In this paper, we propose a serial dilution microfluidic chip which is able to generate logarithmic or linear step-wise concentrations. These concentrations were generated *via* adjustments in the flow rate of two converging fluids at the channel junctions of the ladder network. The desired dilution ratios are almost independent of the flow rate or diffusion length of the molecules, as the dilution device is influenced only by the ratio of volumetric flow rates. Given a set of necessary dilution ratios, whether linear or logarithmic, a serial dilution chip can be constructed *via* the modification of a microfluidic resistance network. The design principle was suggested, and both the logarithmic and linear dilution chips were fabricated, in order to verify their performance in accordance with the fluorescence intensity. The diluted concentrations of a fluorescein solution in the microfluidic device evidenced relatively high linearity, and the cytotoxicity test of MCF-7 breast cancer cells via the logarithmic dilution chip was generally consistent with the results generated with manual dilution.

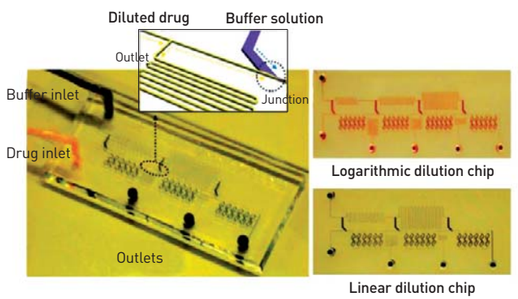

2 A Near-Infrared-Fluorescence-Quenched Gold-Nanoparticle Imaging Probe for *In Vivo* Drug Screening and Protease Activity Determination**

Angew. Chem. Int. Ed., 47, 2008, 2804 -2807

Seulki Lee, Eui-Joon Cha, Kyeongsoon Park, Seung-Young Lee, Jin-Ki Hong, In-Cheol Sun, Sang Yoon Kim, Kuiwon Choi, Ick Chan Kwon, Kwangmeyung Kim, and Cheol-Hee Ahn

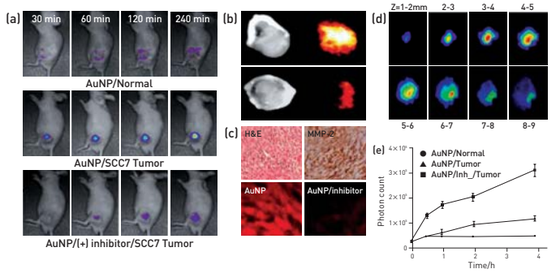

Nanoscale fluorescence optical imaging probes are paving the way for novel methods to sense and spot live molecular targets. Various probes have been developed, including semiconductor quantum dots, magnetofluorescent nanoparticles, polymer conjugates, nanocomplexes, and gold nanoparticles (AuNPs). The application of conventional fluorescent probes is limited because they generally display only modest fluorescence changes, thus providing insufficient resolution. The limited degree of resolution is mainly attributed to the low fluorescence-quenching efficiency and specificity of the probes. Therefore, a high quenching efficiency and specific recognition properties by the target biomolecules are essential for the development of supersensitive fluorescence-based probes. Among the diverse candidates, biocompatible AuNPs offer a considerable advantage in obtaining optical images through their nearinfrared-fluorescence (NIRF) quenching properties. Chromophores in close proximity to AuNPs experience strong electronic interactions with the surface, which result in the donation of excited electrons to the metal nanoparticles and almost perfect quenching of the fluorescence. However, the use of AuNP probes for *in vivo* visual biomolecular detection and real-time fluorescence tomography remains to be explored.

3 Highly Aligned Ultrahigh Density Arrays of Conducting Polymer Nanorods Using Block Copolymer Templates

Nano Letters, 8, 2008, 2315

Jeong In Lee, Shin Hyo Cho, Su-Moon Park, Jin Kon Kim, Jai Kyeong Kim, Jae-Woong Yu, Young Chul Kim, and Thomas P. Russell

Ultrahigh density arrays of conducting polypyrrole (PPy) nanorods are fabricated directly on the indium-tin oxide coated glass by an electropolymerization within a porous diblock copolymer template. The nanorods are shown to have a much higher conductivity than thin PPy films due to the high degree of chain orientation, even though the separation distance for two neighboring PPy main chains is as small as 0.37 nm. The ultrahigh density arrays of conducting polymer nanorods have potential applications as sensor materials, nanoactuators, and organic photovoltaic devices.

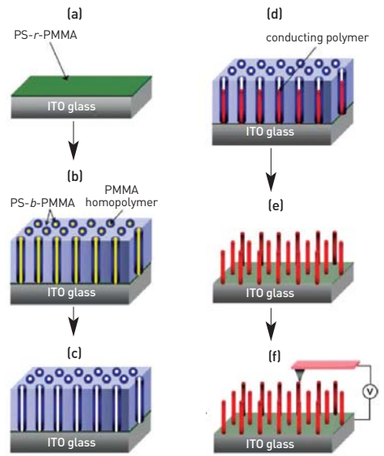

4 Pt-CeO_2/C Anode Catalyst for Direct Methanol Fuel Cells

Applied Catalysis B: Environmental 84, 2008, 773–782

M. Aulice Scibioh, Soo-Kil Kim, Eun Ae Cho, Tae-Hoon Lim, Seong-Ahn Hong, Heung Yong Ha

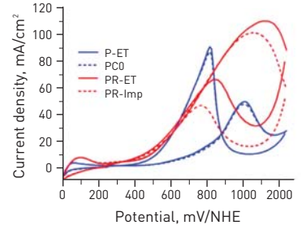

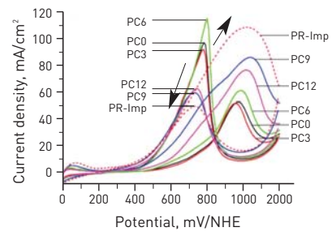

In order to develop a cheaper and durable catalyst formethanol electrooxidation reaction, ceria (CeO_2), as a co-catalytic material with Pt on carbon, was investigated with the aim of replacing Ru in PtRu/C which is considered a prominent anode catalyst to date. A series of Pt-xCeO_2/C catalysts and PtRu/C, were synthesized by a wet impregnation method. Electrocatalytic activities of these catalysts for methanol oxidation were examined by cyclic voltammetry and chronoamperometry techniques. It was found that 40 wt% Pt-9 wt% CeO_2/C catalyst exhibited a better activity and stability than did the unmodified Pt/C catalyst. Hence, we explored the possibility of employing Pt-CeO_2 as an electrocatalyst for methanol oxidation. The physicochemical characterizations of the catalysts were carried out by using Brunauer Emmett Teller (BET) surface area and pore size distribution (PSD) measurements, X-ray photoelectron spectroscopy (XPS), transmission electron microscopy (TEM), and X-ray diffraction (XRD) techniques. A tentative mechanism was proposed for a possible role of ceria as a co-catalyst in Pt/C system for methanol electrooxidation.

5 Influence of Cathode Flow Pulsation on Performance of Roton-exchange Membrane Fuel Cell

Journal of Power Sources 185, 2008, 112–117

Yun Ho Kim, Hun Sik Han, Seo Young Kim and Gwang Hoon Rhee

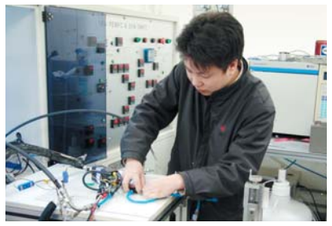

The effect of cathode flow pulsation on the performance of a 10-cell proton-exchange membrane fuel cell is investigated. An acoustic woofer generates a pulsating flow, which is added to a unidirectional flow supplied from a compressed air tank. By adding the flow pulsation, the fuel cell power output and the limit current dramatically increase while the fuel cell efficiency slightly decreases. As the pulsation amplitude increases, the improvement in fuel cell performance is more pronounced. The performance enhancement shows no obvious dependency on a pulsation frequency change from 10 to 30 Hz. The cathode flow pulsation effect is more distinct at low cathode flow rates.

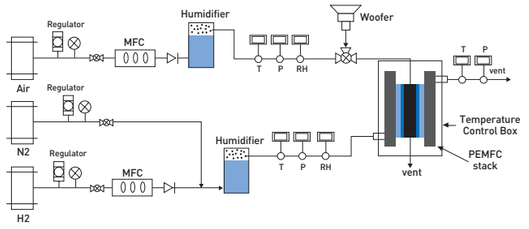

6 Tuning Thalamic Firing Modes Via Simultaneous Modulation of T- and L-Type Ca^{2+}Channels Controls Pain Sensory Gating in the Thalamus

The Journal of Neuroscience, 28, 2008, 13331-13340

Eunji Cheong, Sukchan Lee, B. Jiwon Choi, Minjeong Sun, C. Justin Lee, and Hee-Sup Shin

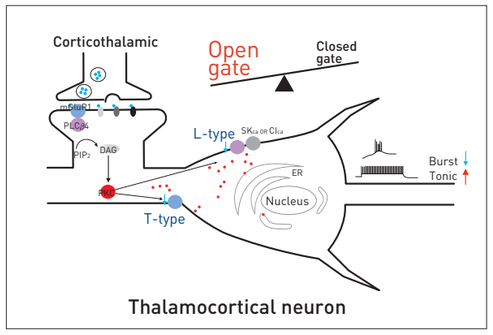

Thalamocortical neuron

Two firing modes of thalamocortical (TC) neurons, tonic and burst firings, are thought to reflect the divergent states of sensory signal transmission from the thalamus to the cortex. We demonstrate that burst and tonic firings of TC neurons are concomitantly regulated by PLCβ4-PKC pathway via simultaneous modulation of T- and L-type Ca^{2+} channels. The mice with increased bursting and decreased tonic firing of TC neurons showed reduced visceral pain responses. Our study also highlights the thalamic PLCβ4-PKC pathway as a "molecular switch" for the firing modes of TC neurons and thus for pain sensory gating.

PATENTS

PHOTO-ELECTRODES EQUIPPED MESO POROUS METAL OXIDE LAYER FOR DYE-SENSITIZED PHOTOVOLTAIC CELL AND METHOD FOR PREPARING THE SAME

Patent No. KR 10-0838158 Contact Info. **Park, Nam-Gyu** (npark@kist.re.kr)

This patent discloses a photo-electrode for a dye-sensitized solar cell comprising a meso-porous metal oxide thin film formed on the surface of the conductive substrate.

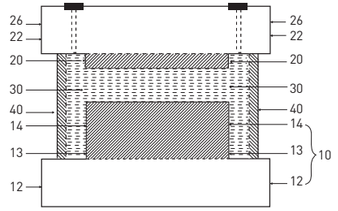

WATER-COOLED GRATE

Patent No. US 7,426,892 Contact Info. **Jurng, Jong Soo** (jjurng@kist.re.kr)

The grate body is formed with a portion for receiving the cooling pipe and a heat transfer controlling member fixed to the pipe-receiving portion for increasing and decreasing the heat transfer between the grate body and the cooling pipe by varying thermal resistance to the cooling pipe through thermal deformation according to the temperature change of the grate body.

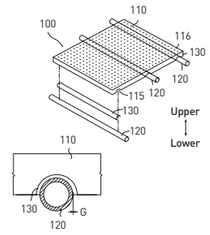

HEAT RESISTING SEPARATOR HAVING ULTRAFINE FIBROUS LAYER AND SECONDARY BATTERY HAVING THE SAME

Patent No. KR 10-0845239 Contact Info. **Jo, Seong-Mu** (smjo@kist.re.kr)

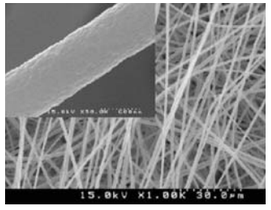

This patent discloses a polyolefin separator with a heat-resistant ultrafine fibrous layer and a secondary battery using the same. Accordingly, this separator is particularly useful for electrochemical devices used in hybrid electric automobiles, electric automobiles, and fuel cell automobiles, all of which require high thermal endurance and thermal stability.

METHOD FOR PREPARING ZnO NANOCRYSTALS DIRECTLY ON A SILICON SUBSTRATE

Patent No. KR 10-0835666 Contact Info. **Cho, Woon Jo** (woonchoj@kist.re.kr)

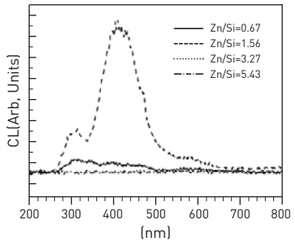

This patent shows a method for preparing a ZnO nanocrystal directly on a silicon substrate. With this invention method, more applications of ZnO nanocrystals in optoelectronic devices using a silicon substrate are possible.

DEHUMIDIFYING ELEMENT AND MANUFACTURING METHOD FOR THE SAME

Patent No. US 7,326,363 Contact Info. **Lee, Dae-Young** (ldy@kist.re.kr)

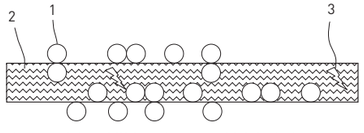

This patent discloses a dehumidifying element which includes a super absorbing polymer (SAP) and a hygroscopic base, thereby maintaining hygroscopic characteristics, regardless of aging, and a high humidity absorbing rate requiring a smaller amount of energy for regeneration.

1,3-DIOXOISOINDOLE DERIVATIVES WITH SELECTIVE ANTAGONISM OF T-TYPE CALCIUM CHANNEL

Patent No. US 7,319,098 Contact Info. **Cho, Yong Seo** (ys4049@kist.re.kr)

The present invention relates to 1,3-dioxoisoindole derivatives of Formula (1), and use as a T-type calcium channel antagonist. 1,3-dioxoisoindole derivatives of Formula (1) show selective antagonistic activity against a T-type calcium channel, thus being effective in treating brain diseases, cardiac diseases, and neurogenic pains.

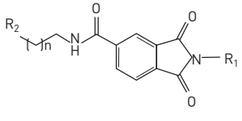

KIST News

KIST and KAERI to Cooperate in the Establishment of a High Resolution Small Angle Neutron Scattering (HR-SANS) Center

Construction of a high resolution small angle neutron scattering (HR-SANS) center will serve as a basic science research hub in Korea. KIST and the Korea Atomic Energy Research Institute (KAERI) held a technology cooperation ceremony at KAERI in Daejeon on November 27, 2009, pledging to work together in the establishment of a high resolution small angle neutron scattering (HR-SANS) center. KIST is investing 2.3 billion won in the project. KIST expects this cooperation with KAERI to not only benefit research by KIST scientists, but also to contribute significantly to the development of neutron science in Korea. With the establishment of an HR-SANS center, KIST will have a world class infrastructure for analysis equipment on a large scale similar to its previously announced projects involving the X-ray beamline established at the Pohang Accelerator Laboratory, the 900MHz NMR, 200kV Cryo-TEM, and 6MV tandem ion beam accelerator, projects which are to be completed by 2011. The world class analysis equipment infrastructure of KIST will function as Korea's basic science research hub leading to advances in understanding interdisciplinary fundamental principles in the fields of material science, the environment, energy, biology, physics, and chemistry.

KIST and NIMS of Japan Sign MoU for Mutual Cooperation

Dr. Dongwha KUM, President of KIST, invited Dr. Teruo KISHI, President of the National Institute of Materials Science (NIMS) to KIST on August 28, 2008, and initiated an agreement for mutual cooperation between the two institutions. A policy seminar was also held at that time exploring the theme of "Japan's R&D Strategy for Nanotechnology/Materials and NIMS Activity." As evidenced by this agreement, both institutions recognize the importance of research cooperation related to the parts and materials industry, an area at the heart of the trade imbalance between Korea and Japan. Both KIST and NIMS are planning to organize regular symposia for identifying joint research projects in areas of original technology. On August 27, 2008, both Dr. Dongwha KUM and Dr. KISHI delivered keynote speeches at the NANO KOREA 2008 event which was held at the KINTEX and exchanged views about the direction of future research.

KIST and 360ip Conclude an Agreement for Technology Commercialization

360ip will invest $20 million over five years for technology commercialization. It will carry out the regular technology commercialization preferentially for local companies. Dr. Dongwha KUM, President of KIST, signed an agreement for technology commercialization with 360ip, a financial technology company established by Battelle Memorial Institute (BMI) and Battelle Ventures. Battelle Memorial Institute is the world's largest non-profit research organization.According to the terms of this agreement, 360ip will invest $20 million over five years in commercializing KIST's original technology including about 1,500 patents developed by KIST in the fields of material, computer, energy, robot and life sciences. Assistance from 360ip will make the most of Battelle's human resource capabilities, technology evaluation systems, and extensive experience in technology commercialization. 360ip is also planning to carry out joint technology commercialization with KIST by coordinating the patents and technology of renowned research institutes in its partnership network.

Korea-Germany Nanophotonics Workshop Held in Buddhist Temple

The 4th Korea-Germany Nanophotonics Workshop, organized by KIST's Nano Device Research Center, was held at Bongin Temple, Namyangju, October 5-7, 2008. The workshop addressed a scientifically and economically important area of nanotechnologies related to information technology. At this workshop, German and Korean experts were brought together to exchange information and discuss novel aspects of this very active field of international research. Discussions included a review of the state of the art in nanophotonics based on quantum dots, photonics crystals and metamaterials, and direct collaborations were initiated in the form of joint projects including exchanges of scientists and students. The first workshop was held in Berlin (2005), followed by ones in Seogwipo (2006) and Rothenburg (2007). Attending the workshop were seven German experts from different universities led by Prof. A. Forchel of Wuerzburg University who also participated in the Temple Stay Program with meditation lessons and dawn worship requiring 108 deep bows in keeping with traditional Korean culture.

Korea-Italy Bilateral Workshop Held on Photonics for Communications and Sensing

Named the "Year of Italy in Korea," 2008 marked a time when Italy renewed its commitment to a strong relationship with Korea. Both countries are giving special attention to science and research, an area offering many opportunities for successful co-operation. On October 23-24, 2008, at the Shilla Hotel, KIST held a Korea-Italy Bilateral Workshop on Photonics for Communications and Sensing with Scuola Superiore Sant'Anna. At the workshop, many distinguished representatives from the two countries (13 Italian and 14 Korean participants) presented photonics issues of current significance. The workshop served as an excellent platform for participants to learn more about the latest scientific and technical advances in the field, share knowledge and opinions, and at the same time, get to know each other. Photonics promises to be the technology of the 21st century, just as electronics was for the 20th. Through this advanced technology, photons (light) can replace electrons in collecting, processing and transferring information, with potential applications in various fields. Telecommunications and sensing is one of these fields and was the focus of this workshop whose purpose was to promote a productive interaction among researchers and scientists from both Korea and Italy. Representatives from industry, academia, and research institutions were brought together to discuss issues and compare the latest results, experiences, plans and achievements generated by applying photonics to the telecomunications and sensing field.

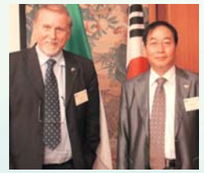

1st Workshop for International Standardization of Diamond-like Carbon Coatings

A workshop to classify the diamond-like carbon (DLC) coating of various atomic structures and properties was held on Jeju Island, Korea, from Oct. 1-3, 2008. This workshop, co-chaired by Dr. Kwang-Ryeol Lee of KIST (Korea), Prof. Hidetoshi Saitoh of Nagaoka University of Technology (Japan), and Dr. Klaus Bewilogua of Fraunhofer Institute of Surface Technology (Germany), represented the first step for global standardization of DLC coatings. At this workshop, the following issues were discussed.

1. Review of the present status of DLC standardization in Germany and Japan.
2. Identification of industry requirements.
3. Identification of the key parameters for classification of DLC coating.
4. Specification of the characterization tools for the classification of DLC coating.

38 participants from Korea, Japan, China, Taiwan, Singapore and Germany took part in valuable discussions on the present status of DLC coating and its industrial applications. One of the most significant results of this workshop was the suggestion that the classification be considered in terms of the properties and areas of application.

Awards

- **Dr. Yong Su Choi, Center for Environmental Technology Research**
  - Presidential Commendation (Ministry of Public Administration & Security, March 21, 2008)
- **Dr. Dong Seok Lho, Bioanalysis & Biotransformation Research Center**
  - Order of Science and Technology Merit Award (Ministry of Education, Science and Technology, April 21, 2008)
- **Dr. Wan Cheol Park, Center for Environmental Technology Research**
  - Science and Technology Merit Medal (Ministry of Education, Science and Technology, April 21, 2008)
- **Dr. Jung Il Lee, Nano-Devices Research Center**
  - Prestigious Academic Palm Medal Knight (French Government, May 19, 2008)
- **Dr. Tae Song Kim, Intelligent Microsystems Center**
  - Media and Culture Award (Maeil Business Newspaper, July 10, 2008)
- **Dr. Il Doo Kim, Center for Energy Materials Research**
  - The 17th Da-San Technology Award (September 10, 2008)
  - DaVinci Award - Young Scientist (Korean Research Council for Fundamental Science and Technology, December 29, 2008)
- **Dr. Young Sook Yoo, Life Sciences Research Division**
  - AMOREPACIFIC Grand Prize (October 29, 2009)
- **Dr. Sang Rok Oh, Center for Cognitive Robotics Research**
  - Prime Minister's Commendation (Ministry of Knowledge Economy, December 3, 2008)
- **Dr. Hee-Sup Shin, Center for Neural Science**
  - Cornell Club of Korea Award (December 7, 2008)
- **Dr. Nam-Gyu Park, Solar Cell Research Center**
  - Scientist of the Month (Korean Science Foundation, October 13, 2008)
  - Prime Minister's Commendation (Kyunghyang Daily, December 17, 2008)
  - Korea Technology Award (Korea Industrial Technology Foundation, December 22, 2008)
- **Dr. Byung Won Cho, Battery Research Center**
  - Presidential Commendation (Ministry of Education, Science and Technology, December 26, 2009)

A Sign of Times!

2009 marks the 43rd anniversary of the founding of KIST. The history of the institute, and the changes that it (and the country) have undergone are reflected in the various KIST logos used over the years. To date, there have been five logos, all representative of the eras in which they were designed.

1966

KIST's first logo, designed for its founding in 1966, paid homage to the Korean alphabet (Hangul), while also using English. The top half illustrates (in Hangul) the "han" (K) for the first letter of Korea, the "kwa" (S) for the first letter in science, and the "yun" (I) for the first letter of institute. Beneath it lies a stylized version of "KIST." This logo represents the beginning of the institute.

1967-1980

After only five months, a second logo replaced the first, but it was retained for 13 years. Of the five logos, it is the only one that is actually a symbol and emphasizes the purpose behind the establishment of KIST. In the center is the symbol of three-fold crystal symmetry, representing the world of science, the driving force behind the development of industry and technology. It is surrounded by a gear, which represents industry and practical technologies. This logo was developed to symbolize the purpose and goals of KIST during the period of industrial development in Korea.

1981-1989

1981 brought about a change in attitude and direction at KIST with an emphasis on education. The logo was developed to embody the perfect harmony of KIST's dual functions as an educational institute as well as a research institute. In the center of the logo, the letter "S" can be seen, for science. The letter "kiyuk," the first letter in Hangul for both science and technology, was the inspiration for this choice. Kiyuk is used as a mirror image of itself in the logo and when mirrored again at an angle, the "S" appears. The colors used in the logo have meaning as well: the cerulean blue represents the education of talented scientists and their dreams for their own research potential; the cobalt blue suggests deep wisdom.

1989-2003

The next change in the logo appeared in 1989. At that time, the image of scientists in Korea was not terribly positive, so this logo set out to change that perception. The square shape epitomizes the well-structured organization of research activities as well as the integrity and commitment of the scientists. The elongated dot on the "I" exemplifies infinity - the infinite dedication and passion of the researchers.

2003- Now

The latest KIST logo is one of passion, power, and leadership as exhibited in the color red. The staggering of the letters may appear chaotic, but there is order in the chaos, as epitomized by the words of Henry Brooks Adams: "In plain words, Chaos was the law of nature; Order the dream of man." The staggering reflects versatility, flexibility, and individuality. The prominence of the letter "I" is associated with the number "1" personifying "The Best," "Number 1," pre-eminence, and paramount accomplishments. This current logo is intended to reflect KIST's reputation as the leader of science and technology research in Korea.

Editorial Information

Editor-in-Chief
B. Hong Kim
Kil-Choo Moon

Editorial board members
Kwang-Ryeol Lee
Jungil Lee
Heedong Ko
Eun Gyeong Yang
Young-Woong Suh

Managing Editor
Sehwan Won
kistoday@kist.re.kr

Editorial office telephone
+82-2-958-6161

Web addresses
www.kist.re.kr
www.kist.re.kr/en

English Advisory Services
Anne Charlton

The Final Word Editing Services
the_final_word@live.com

Korea Institute of Science and Technology
Cheong Ryang, P.O. Box 131, Seoul 136-650, South Korea